11th U. S. National Combustion Meeting
Organized by the Western States Section of the Combustion Institute
March 24-27, 2019
Pasadena, California

Numerical Study on Direct Injection of Hydrogen-Methane Blends into a Constant Volume Combustion Chamber

Martia Shahsavan[1,], Mohammadrasool Morovatiyan[1], John Hunter Mack[1]*

[1]Department of Mechanical Engineering, University of Massachusetts Lowell, One University Ave, Lowell, MA, USA
[*]Corresponding Author Email: martia_shahsavan@student.uml.edu

Abstract: Natural gas is not commonly used in compression ignition cycles due to difficulty in achieving autoignition conditions. The addition of hydrogen to natural gas can help overcome this issue considering hydrogen's flammability range and ability to autoignite. In this computational study, the turbulent injection of hydrogen-methane mixtures with varied composition of the gaseous fuels into a constant volume combustion chamber has been modeled. All conditions including injection pressure, initial chamber temperature, and initial chamber pressure are kept constant; the jet properties and combustion characteristics were then investigated. The results indicate that adding hydrogen to methane drastically shortens the ignition delay, enables the system to run at a lower initial temperature, and provides appropriate conditions for the compression ignition of the gaseous fuel. Increasing the volume fraction of hydrogen in the mixture strongly affects the spray tip penetration length and cone angle, while altering the mixing rate of the injected fuel with air. The mixtures with higher hydrogen volume fractions penetrate more during the early stages of injection. However, the higher momentum of the mixtures with more methane compensates for this effect when the jet disperses significantly in the chamber.

Keywords: Natural Gas, Hydrogen, Compression Ignition, Gaseous Combustion, Direct Injection

1. Introduction

Natural gas has a low carbon to hydrogen ratio compared to common transportation fuels, which leads to a reduction of carbon dioxide, carbon monoxide, and unburned hydrocarbons emissions in combustion applications. A large number of studies call it the cleanest fossil fuel on earth, which motivates further investigation for use in transportation and internal combustion engines, specifically [1, 2]. There are more than 200 trillion cubic meters (TCM) of natural gas reserves in the world, and United States possesses roughly 10 TCM which is the fourth after Russia, Iran, and Qatar [3]. Natural gas has a relatively high octane number (about 120) compared to gasoline and is therefore more resistant to autoignition and knock. Thus, it provides the possibility of running the engine at increased compression ratios, which leads higher efficiencies. The utilization of natural gas in premixed combustion, such as spark ignition systems, has been extensively studied [4-9].

The direct injection of fuels provides an increased ideal thermodynamic efficiency as a result of running the engine at a higher compression ratio. Moreover, it prevents backfire in the intake manifold, which is a common problem in spark ignition systems [10]. The use of natural gas in

nonpremixed combustion such as compression ignition cycles is quite limited due to its extremely low cetane number and difficulty in achieving autoignition. Several research groups have attempted to tackle this issue by simultaneously using other fuels with a high cetane number such as diesel [11-14]. In a recent study, methyl propanoate, a biodiesel surrogate, has been introduced as an efficient additive for methane to drastically decrease the ignition delay [15]. In another work, replacing the working fluid with a lower specific heat gas such as argon has been indicated an effective solution for the use of natural gas in compression ignition cycles [16].

Hydrogen is a potential alternative fuel for use in internal combustion engines, as it considerably reduces the amount of major pollutants such as carbon monoxide, carbon dioxide, and unburned hydrocarbons due to the elimination of carbon atoms in the fuel stream [17, 18]. Furthermore, it has a broad flammability range of 4-75% in air. Considering global warming and the limited amount of fossil fuel reserves, hydrogen can be a leading renewable fuel in the near future [19]. A number of studies have investigated the use of hydrogen in spark ignition and compression ignition engines both numerically [20-22] and experimentally [23-26].

A mixture of hydrogen and methane, as the main component of natural gas, can be advantageous since these two gaseous fuels are complementary and cover the drawbacks of each other. Hydrogen helps methane in autoignition issues, improves the combustion stability, increases the upper exhaust gas recirculation limit (which results in lower NOx emissions), decreases cycle to cycle variation, and introduces H and OH radicals that boost the combustion reactivity. Methane, on the other hand, is able to regulate the ignition timing, flame speed, and temperature range. Additionally, it allows for higher compression ratios due to its high octane number [27]. A number of studies have explored the capabilities of hydrogen-methane mixtures in a constant volume chamber [28], spark ignition engines [29-31], compression ignition engines [32], and as a turbulent hot jet [33]. In this paper, the direct injection of different hydrogen-methane blends is numerically studied in a Constant Volume Combustion Chamber (CVCC) and the combustion characteristics, such as ignition delay and jet properties, are compared.

2. Methods

Numerical Modeling

In this numerical study, the direct injection of methane-hydrogen blends into a CVCC is modeled using the CONVERGE software package to investigate the effect of hydrogen addition to methane on ignition delay, jet penetration length, and spray cone angle. The domain is separated into three different regions involving specific operating conditions. The first region includes the fuel at 80 bar and 450 K. It is assumed that the continuous flow of the fuel is entering this region as a pressure-inlet boundary condition at 80 bar. The second region is the nozzle with a no-slip wall boundary condition. The CVCC is the third region, containing air (21% oxygen, 79% nitrogen) at an initial pressure of 20 bar and an initial temperature ranging from 1100 K to 1500 K. The geometry and details of the chamber, nozzle, and injector are shown in Figure 1.

CONVERGE has the advantage of automatic orthogonal high-quality mesh generation. In this modeling, the base grid size is set at 0.5 mm. As shown in Figure 1, a fixed embedding of scale 4 is applied to the nozzle region to predict an accurate inlet velocity profile. A second fixed embedding of scale 3 is applied to a part of the domain where the injected fuel has a high velocity (near nozzle), and a relatively fine grid is required. To avoid the high computational

cost, adaptive mesh refinement (AMR) is applied on velocity and temperature with maximum 2 embedding levels, and the upper limit of refinement is set to 2 million cells. Chamber specifications and boundary conditions are shown in Table 1. A varied time step with a minimum size of 1e-7 seconds is selected for the transient simulation.

Table 1. Chamber specifications and boundary conditions

Parameters	Specifications
Chamber length	50 mm
Chamber diameter	20 mm
Fuel	Methane-hydrogen blends
Hydrogen concentration in fuel	0, 25, 50, 75% by volume
Oxygen concentration in air	21% by volume
Initial pressure of the chamber	20 bar
Initial temperature of the chamber	1100, 1200, 1300, 1400, 1500 K
Injection pressure	80 bar
Fuel temperature	450 K
Nozzle diameter	1 mm

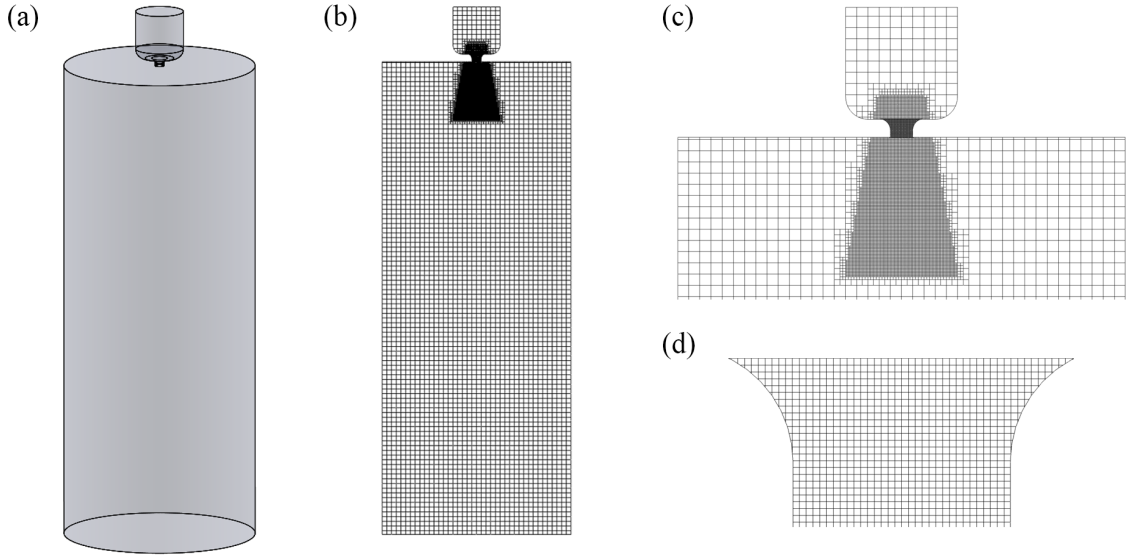

Figure 1. (a) Geometry of the model, (b) Grid configuration on a slice of the model, (c) Fixed embedding on the nozzle (scale 4) and near nozzle areas (scale 3), (d) Grid configuration on the nozzle (31.25 μm).

The Redlich-Kwong equation of state, which is generally more accurate than the ideal gas equation at temperatures above the critical temperature, is selected for the gas simulation model. A reduced version of GRI-Mech including 24 species and 104 reactions is used for the chemical kinetics mechanism in this simulation. For combustion modeling, SAGE detailed chemistry solver of CONVERGE is utilized to calculate the reaction rates at specified temperatures and pressures. In direct injection of gaseous fuels, the high speed flow of the jet produces a huge momentum, which leads to mixing with air. Therefore, an appropriate turbulence model is required to ensure accuracy. In this study, a Reynolds Averaged Navier-Stokes (RANS) model is used to calculate the kinetic energy (k) and dissipation rate (ε).

Ignition Delay, Penetration Length, and Cone Angle Measurement

To investigate the nonpremixed combustion of methane-hydrogen blends, ignition delay is measured and compared for different mixtures at identical operating conditions. Ignition delay is defined as the time interval between the start of injection and the onset of combustion (i.e. ignition). There are several methods for the measurement of ignition delay [34]. In this study, the history of the maximum temperature is used to calculate the ignition delay by extrapolation of the steepest slope of the curve to the initial temperature.

Penetration length and cone angle are two parameters for evaluating the direct injection of fuels. Penetration length is defined as the distance between the nozzle and the tip of the jet. Once the fuel is injected, the air entrainment results in mixing with the fuel. Therefore, the jet propagates in radial directions and creates a cone shape. In this study, the jet penetration length and cone angle for nonreacting cases are calculated using image processing on contours of mixture fraction in MATLAB. First, a grayscale filter is applied on images. Then, the pixel intensity of the points on the injection axis are plotted. In this plot, 0 represents pure black and 255 represents pure white. The first point at which the pixel intensity drops below a certain value (10 here) is marked as the jet tip, and its distance with the nozzle is calculated and assigned as the jet penetration length. For cone angle, the edge of the jet is detected using several filters, and then the cone angle is calculated based on the location of the points at maximum distance to the injection axis. The details of the image processing mentioned above can be found in the previous studies [16, 20].

3. Results and Discussion

Ignition Delay

In nonpremixed combustion applications such as compression ignition cycles, ignition delay can be used as a crucial parameter in evaluating the autoignition of the fuel. In this study, four different blends of methane and hydrogen (0, 25, 50, 75% hydrogen by volume) are injected at 80 bar and 450 K into air at 20 bar. In order to assess the ignition delay of the mixtures at different initial temperatures, 5 cases with initial temperatures of 1100, 1200, 1300, 1400, and 1500 K are modeled. The maximum temperature at each time step is recorded and plotted in Figure 2. Each mixture is shown in a specific color, and the different line types distinguish the initial temperature. The rapid rise of the temperature curves is the result of the ignition. Due to the wide timescale of the cases, the x-axis which shows the time is displayed in logarithmic scale.

Figure 2 indicates that increasing the volume fraction of hydrogen in the mixture drastically advances the ignition timing. Pure methane (0% hydrogen) at 1100 K ignites at about 8.3 ms, while adding 25% hydrogen accelerates the ignition timing to 4.6 ms, which is quite close to the ignition delay of pure methane at 100 K higher initial temperature. Increasing the hydrogen fraction in the mixture to 50% decreases the ignition delay to about 3 ms, and 75% hydrogen blend ignites at about 2 ms, which is quite comparable to the ignition timing of pure methane at 200 K higher initial temperature (1300 K). Ignition timing of 75% hydrogen blend at 1300 K is almost equal to that of 50% hydrogen at 1400 K (both have ignition delay of 0.057 ms), and much smaller than pure methane at 1500 K (0.37 ms). Even 25% hydrogen blend at 1500 K has a longer ignition delay (0.09 ms).

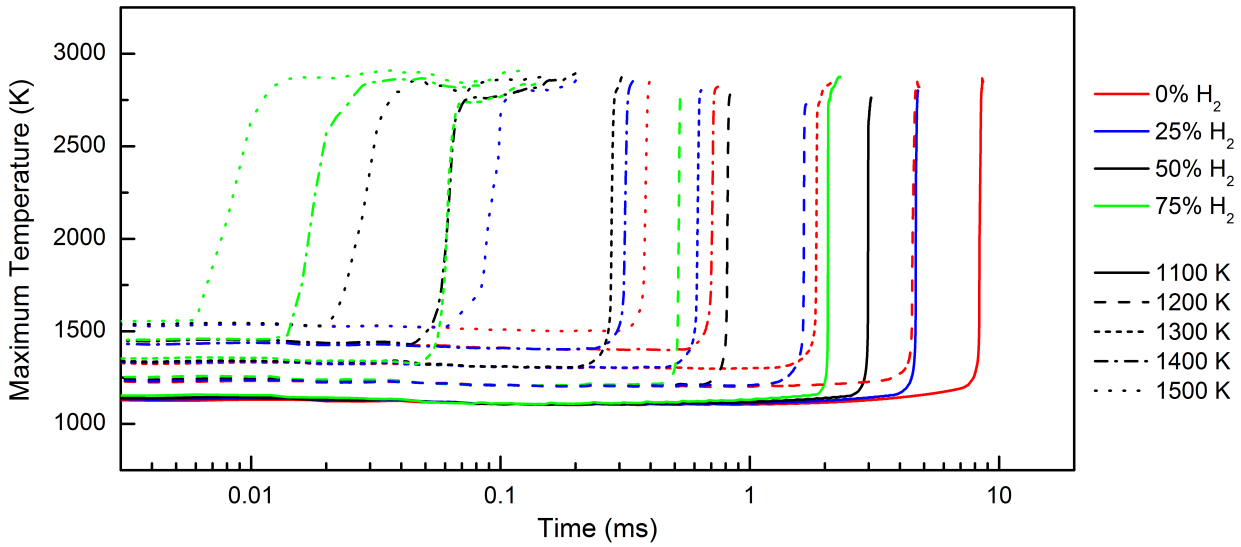

Figure 2. History of maximum temperature for different blends of methane and hydrogen at a range of initial temperature (1100 - 1500 K)

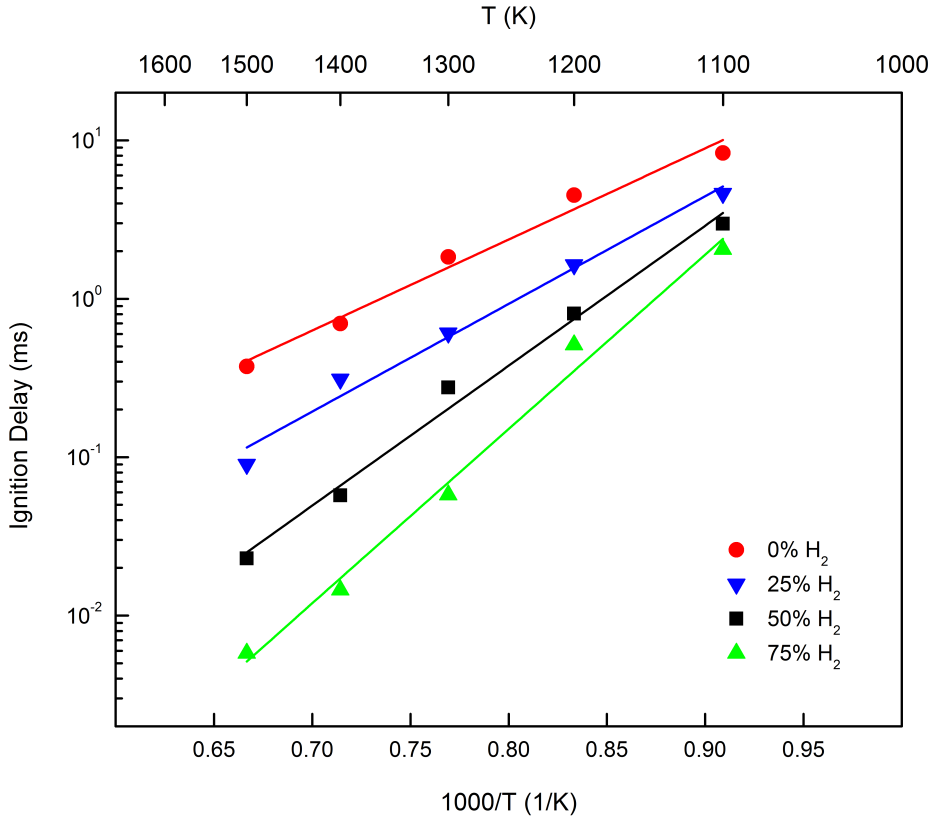

Figure 3. Ignition delay versus initial chamber temperature for different blends of methane and hydrogen

In order to have a clearer impression of the ignition timing of the 20 cases mentioned above, ignition delay in logarithmic scale versus 1000/T is plotted in Figure 3. This is a traditional way of studying the ignition delay since it shows a linear behavior with respect to the reciprocal of the temperature. Figure 3 shows that increasing the initial temperature has a linear reverse

relation to the ignition delay as expected. It also indicates how addition of hydrogen can aid the autoignition issues of methane. At low temperatures, the ignition delay of the 75% hydrogen blend is almost 10 times shorter than that of pure methane. At high temperatures, the ignition delay of the 75% hydrogen blend is almost 100 times shorter than that of pure methane. If a compression ignition cycle is designed based on a temperature of 1100 – 1200 K at top dead center, and an ignition delay of about 1 ms is required, adding only 25% hydrogen to methane can create an appropriate fuel. On the other hand, in a high temperature compression ignition cycle such as the argon cycle [35], adding 25% hydrogen at 1500 K or 50% hydrogen at 1400 K or 75% hydrogen at 1300 K leads to an ignition delay of less than 0.1 ms.

Jet shape

Five different mixtures (0, 25, 50, 75, 100% hydrogen) at 1100 K initial temperature and 20 bar initial pressure are modeled to investigate the behavior of the nonreacting gaseous jets. Figure 4 shows the calculated penetration length and cone angle versus time for the mixtures mentioned above.

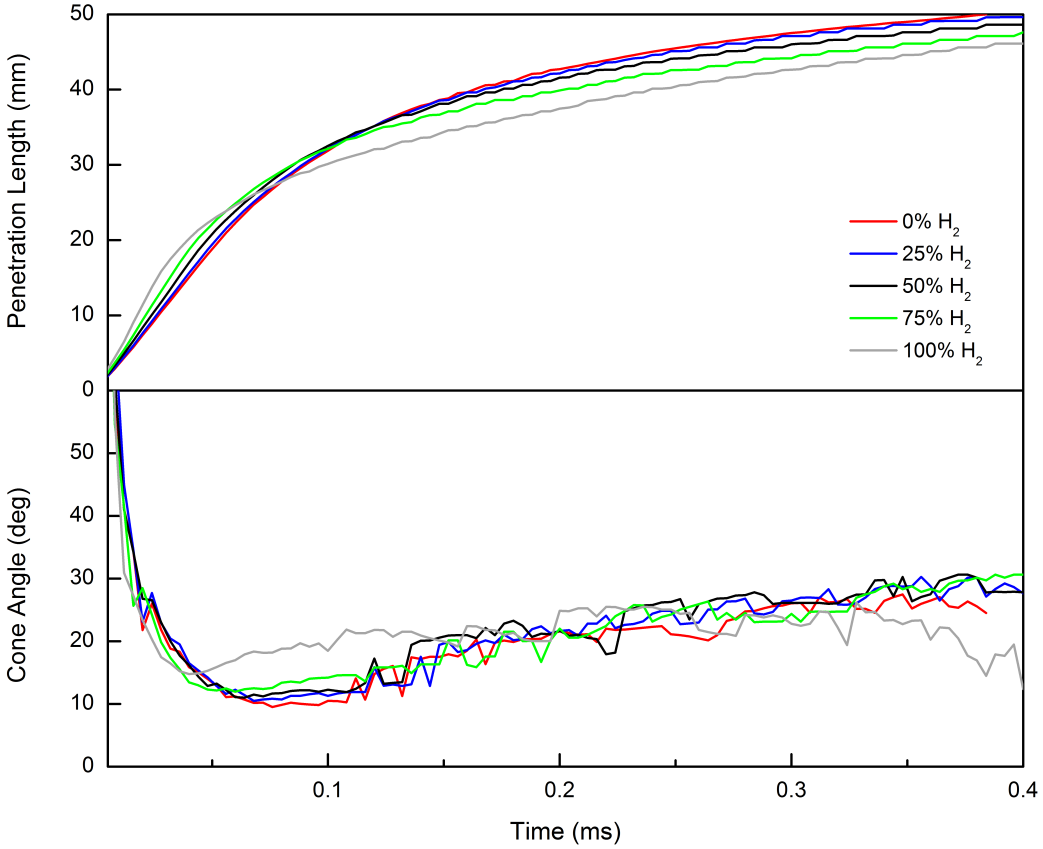

Figure 4. Penetration length and cone angle for different blends of methane and hydrogen

Quite early after injection, the pure hydrogen jet possesses the highest penetration length among the mixtures, and the penetration length decreases with methane addition. However, the correlation between the percentage of hydrogen and the penetration length becomes inverse after a while, and pure methane surpasses the other jets. The cone angle plot shows larger angles for mixtures with higher hydrogen volume fraction at the early stages after injection, while after a significant penetration of fuel in the chamber, the pure hydrogen possesses the smallest cone

angle among the mixtures. In order to explain this behavior, the velocity, momentum per unit volume (ρV), and mixture fraction along the injection axis at three different times after the injection are calculated and plotted in Figure 5. The horizontal axis represents the distance from the nozzle which has a value of 0 at the nozzle tip. This means that the negative values show the injector, and the positive values are related to the chamber.

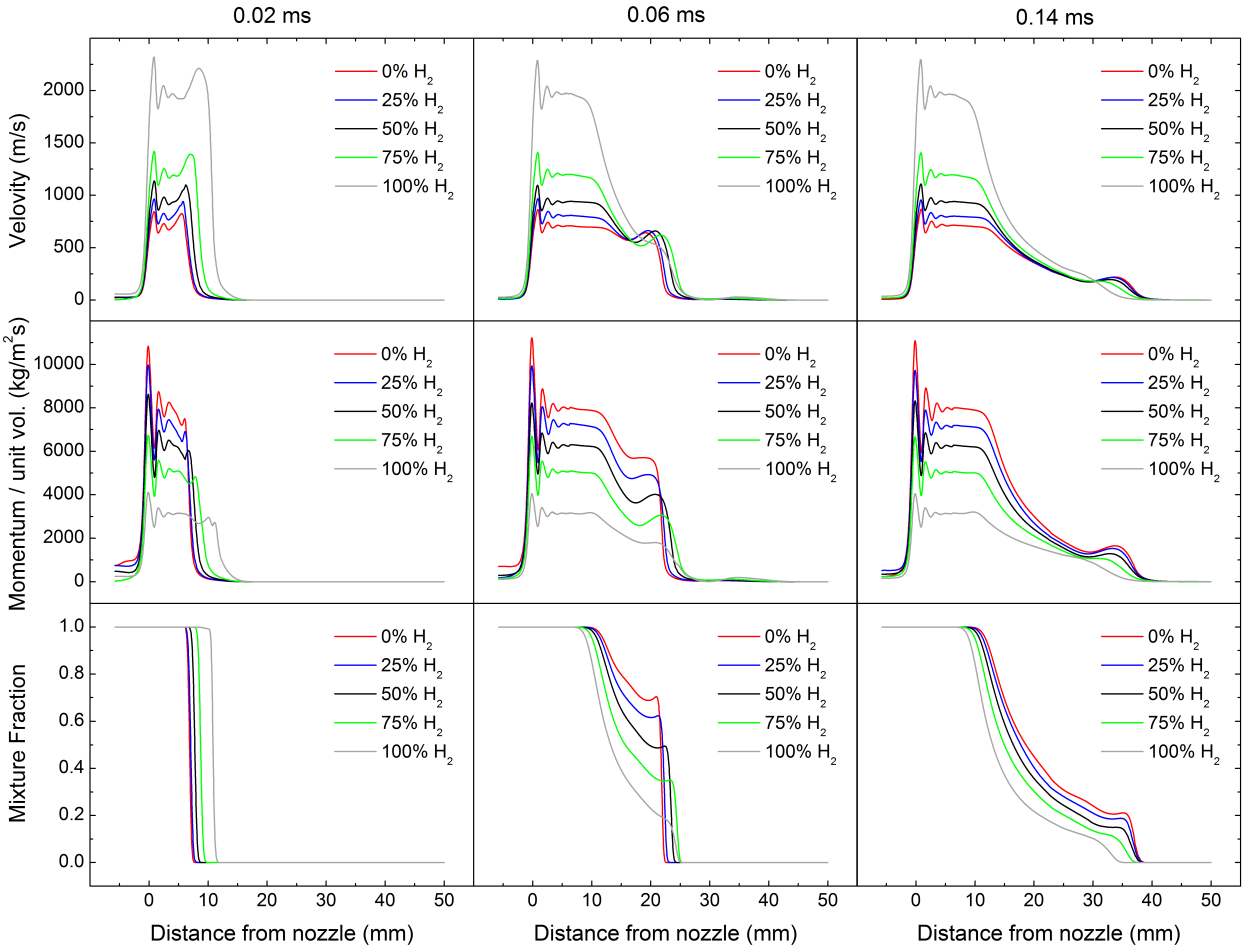

Figure 5. Velocity, momentum per unit volume, and mixture fraction along the injection axis for different blends of methane and hydrogen at 0.02, 0.06, and 0.14 ms after injection

Figure 5 shows velocity, momentum per unit volume, and mixture fraction at 0.02 ms when pure hydrogen possesses the highest penetration length, at 0.06 ms when the mixtures have a relatively comparable penetration length, and at 0.14 ms when the pure methane jet becomes the longest. Noticing the velocity profiles, the pure hydrogen jet has a much higher velocity due to the lower density, and adding methane which increases the jet density leads to the lower axial velocity. The plots in the second row are the velocity magnitudes along the injection axis times density of the jet (ρV) which is called momentum per unit volume. As seen, pure hydrogen has a lower momentum per unit volume compared to the other mixtures. However, the high velocity of the jet near nozzle is still dominant, which helps the jet penetrate more into the air. The third row in Figure 5 shows the mixture fraction along the injection axis, which can be interpreted as the jet penetration. At 0.02 ms, the mixture fraction of the pure methane jet falls in a closer location

to the nozzle compared to its counterparts, which leads to a shorter penetration length. For comparison of the jet shapes at these three selected times, the contours of mixture fraction are illustrated in Figure 6. It is visually clear that hydrogen penetrates more at early periods after injection, which agrees with the plots in Figure 5. The second column plots show the axial velocity, momentum, and mixture fraction at 0.06 ms. At this time, the higher momentum of the mixtures with a greater volume fraction of methane compensates the lower speed, and all the jets have a similar location of mixture fraction drop, which means almost an equal penetration length (see Figure 6 second column). At 0.14 ms when the jets penetrate significantly into the chamber, the effect of momentum dominates velocity, and the mixtures with higher momentum (a greater volume fraction of methane) possess a higher penetration length. Therefore, the hydrogen jet, which has a higher velocity near the nozzle, cannot compete with the other mixtures due to its lower momentum per unit volume, and stays behind them as can be seen in Figure 6.

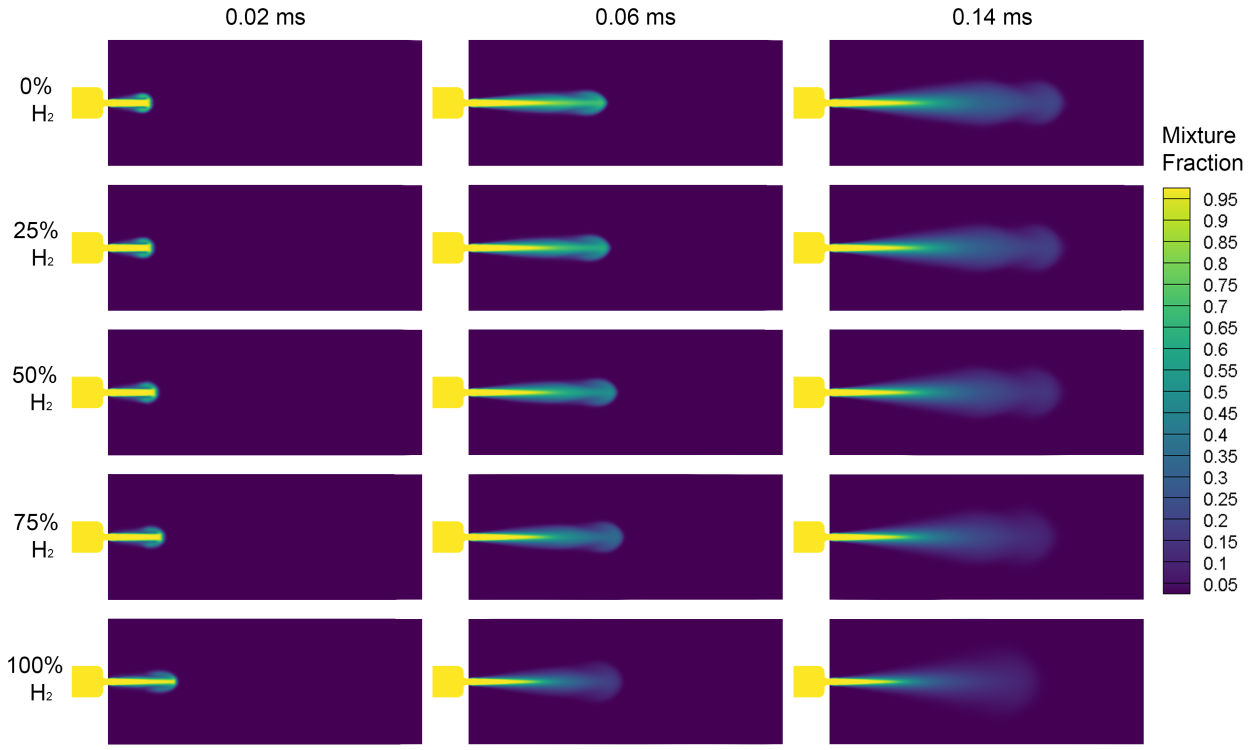

Figure 6. Contours of mixture fraction for different blends of methane and hydrogen at 0.02, 0.06, and 0.14 ms after injection

4. Conclusions

In this paper, the combustion characteristics and jet behavior of methane-hydrogen mixtures injected into air at a constant volume combustion chamber were numerically studied. The following are the outcomes of this study:

- Increasing the volume fraction of hydrogen in the mixture drastically shortens the ignition delay. A 75% hydrogen by volume has roughly an order of magnitude shorter ignition delay than the pure methane at 1100 K. An ignition delay of an order of 0.1 to 1 ms is feasible by using 25-50% hydrogen by volume in the mixture at the initial temperature range of 1100-1300 K.

- The required ignition delay for any compression ignition cycle which is designed for gaseous fuels can be achieved by regulating the ratio of hydrogen to methane.
- The jet shape and penetration are quite different for particular blends of methane-hydrogen. At early times after injection, pure hydrogen possesses a higher penetration length due to its lower density which produces a higher velocity profile near nozzle areas. However, by decreasing the volume fraction of hydrogen in the mixture, the momentum per unit volume increases which compensates the lower velocity near the nozzle. Therefore, a mixture with a higher methane volume fraction penetrates more rapidly after a while compared to its counterparts.

5. Acknowledgements

This research was funded by University of Massachusetts Lowell.

6. References

[1] S. Di Pascoli, A. Femia, and T. Luzzati, "Natural gas, cars and the environment. A (relatively)'clean'and cheap fuel looking for users," *Ecological Economics,* vol. 38, no. 2, pp. 179-189, 2001.

[2] A.-H. Kakaee and A. Paykani, "Research and development of natural-gas fueled engines in Iran," *Renewable and Sustainable Energy Reviews,* vol. 26, pp. 805-821, 2013.

[3] "OPEC annual statistical bulletin," 2015, Available: https://www.opec.org/opec_web/static_files_project/media/downloads/publications/ASB2015.pdf.

[4] A. Kalantari, E. Sullivan-Lewis, and V. McDonell, "Application of a turbulent jet flame flashback propensity model to a commercial gas turbine combustor," *Journal of Engineering for Gas Turbines and Power,* vol. 139, no. 4, p. 041506, 2017.

[5] M. Morovatiyan, M. Shahsavan, M. Shen, and J. H. Mack, "Investigation of the Effect of Electrode Surface Roughness on Spark Ignition," in *ASME 2018 Internal Combustion Engine Division Fall Technical Conference*, 2018, p. V001T03A022: American Society of Mechanical Engineers.

[6] M. R. Boldaji, B. Gainey, and B. Lawler, "Thermally stratified compression ignition enabled by wet ethanol with a split injection strategy: A CFD simulation study," *Applied Energy,* vol. 235, pp. 813-826, 2019.

[7] A.-H. Kakaee, A. Paykani, and M. Ghajar, "The influence of fuel composition on the combustion and emission characteristics of natural gas fueled engines," *Renewable and Sustainable Energy Reviews,* vol. 38, pp. 64-78, 2014.

[8] M. Darzi, D. Johnson, C. Ulishney, and N. Clark, "Low pressure direct injection strategies effect on a small SI natural gas two-stroke engine's energy distribution and emissions," *Applied Energy,* vol. 230, pp. 1585-1602, 2018.

[9] S. Szwaja *et al.*, "Influence of exhaust residuals on combustion phases, exhaust toxic emission and fuel consumption from a natural gas fueled spark ignition engine," *Energy Conversion and Management,* vol. 165, pp. 440-446, 2018.

[10] Y. Kim, J. T. Lee, and G. H. Choi, "An investigation on the causes of cycle variation in direct injection hydrogen fueled engines," *International Journal of Hydrogen Energy,* vol. 30, no. 1, pp. 69-76, 2005.

[11] M. Rahimi Boldaji, A. Sofianopoulos, S. Mamalis, and B. Lawler, "Effect of mass, pressure, and timing of injection on the efficiency and emissions characteristics of TSCI combustion with direct water injection," *SAE technical paper,* pp. 01-0178, 2018.

[12] A. Carlucci, A. d. de Risi, D. Laforgia, and F. Naccarato, "Experimental investigation and combustion analysis of a direct injection dual-fuel diesel–natural gas engine," *Energy,* vol. 33, no. 2, pp. 256-263, 2008.

[13] Z. Wang *et al.*, "Impact of pilot diesel ignition mode on combustion and emissions characteristics of a diesel/natural gas dual fuel heavy-duty engine," *Fuel,* vol. 167, pp. 248-256, 2016.

[14] B. Afkhami, A. Kakaee, and K. Pouyan, "Studying engine cold start characteristics at low temperatures for CNG and HCNG by investigating low-temperature oxidation," *Energy conversion and management,* vol. 64, pp. 122-128, 2012.

[15] S. Jouzdani, X. Zheng, D. M. Coombs, and B. Akih-Kumgeh, "Methane and Methyl Propanoate High-Temperature Kinetics," *Energy & Fuels,* vol. 32, no. 11, pp. 11864-11875, 2018.

[16] M. Shahsavan, M. Morovatiyan, and J. H. Mack, "A Computational Investigation of Non-Premixed Combustion of Natural Gas Injected Into Mixture of Argon and Oxygen," in *ASME 2018 Internal Combustion Engine Division Fall Technical Conference*, 2018, p. V001T03A013: American Society of Mechanical Engineers.

[17] S. Verhelst, "Recent progress in the use of hydrogen as a fuel for internal combustion engines," *international journal of hydrogen energy,* vol. 39, no. 2, pp. 1071-1085, 2014.

[18] S. Verhelst and T. Wallner, "Hydrogen-fueled internal combustion engines," *Progress in Energy and Combustion Science,* vol. 35, no. 6, pp. 490-527, 2009/12/01/ 2009.

[19] K. Mazloomi and C. Gomes, "Hydrogen as an energy carrier: prospects and challenges," *Renewable and Sustainable Energy Reviews,* vol. 16, no. 5, pp. 3024-3033, 2012.

[20] M. Shahsavan, M. Morovatiyan, and J. H. Mack, "A numerical investigation of hydrogen injection into noble gas working fluids," *International Journal of Hydrogen Energy,* vol. 43, no. 29, pp. 13575-13582, 2018/07/19/ 2018.

[21] A. Hamzehloo and P. Aleiferis, "Large eddy simulation of highly turbulent under-expanded hydrogen and methane jets for gaseous-fuelled internal combustion engines," *International Journal of Hydrogen Energy,* vol. 39, no. 36, pp. 21275-21296, 2014.

[22] S. Sukumaran and S.-C. Kong, "Numerical study on mixture formation characteristics in a direct-injection hydrogen engine," *International Journal of Hydrogen Energy,* vol. 35, no. 15, pp. 7991-8007, 2010.

[23] J. G. Antunes, R. Mikalsen, and A. Roskilly, "An experimental study of a direct injection compression ignition hydrogen engine," *International journal of hydrogen energy,* vol. 34, no. 15, pp. 6516-6522, 2009.

[24] P. K. Bose and D. Maji, "An experimental investigation on engine performance and emissions of a single cylinder diesel engine using hydrogen as inducted fuel and diesel as injected fuel with exhaust gas recirculation," *International journal of hydrogen energy,* vol. 34, no. 11, pp. 4847-4854, 2009.

[25] M. R. A. Mansor and M. Shioji, "Investigation of the combustion process of hydrogen jets under argon-circulated hydrogen-engine conditions," *Combustion and Flame,* vol. 173, pp. 245-257, 2016.

[26] J. Naber and D. Siebers, "Hydrogen combustion under diesel engine conditions," *International journal of hydrogen energy,* vol. 23, no. 5, pp. 363-371, 1998.

[27] T. Korakianitis, A. Namasivayam, and R. Crookes, "Natural-gas fueled spark ignition (SI) and compression ignition (CI) engine performance and emissions," *Progress in energy and combustion science,* vol. 37, no. 1, pp. 89-112, 2011.

[28] F. Tinaut, A. Melgar, B. Giménez, and M. Reyes, "Prediction of performance and emissions of an engine fuelled with natural gas/hydrogen blends," *international journal of hydrogen energy,* vol. 36, no. 1, pp. 947-956, 2011.

[29] N. Kahraman, B. Ceper, S. O. Akansu, and K. Aydin, "Investigation of combustion characteristics and emissions in a spark ignition engine fuelled with natural gas–hydrogen blends," *International Journal of Hydrogen Energy,* vol. 34, no. 2, pp. 1026-1034, 2009.

[30] E. Hu, Z. Huang, B. Liu, J. Zheng, and X. Gu, "Experimental study on combustion characteristics of a spark ignition engine fueled with natural gas–hydrogen blends combining with EGR," *International journal of hydrogen energy,* vol. 34, no. 2, pp. 1035-1044, 2009.

[31] M. Bysveen, "Engine characteristics of emissions and performance using mixtures of natural gas and hydrogen," *Energy,* vol. 32, no. 4, pp. 482-489, 2007.

[32] G. P. McTaggart-Cowan, H. Jones, S. N. Rogak, W. K. Bushe, P. G. Hill, and S. Munshi, "Direct-injected hydrogen-methane mixtures in a heavy-duty compression ignition engine," SAE Technical Paper 0148-7191, 2006.

[33] M. E. Feyz, M. R. Nalim, M. N. Khan, A. Tarraf, and K.-Y. Paik, "Three-Dimensional Simulation of Turbulent Hot-Jet Ignition for Air-CH 4-H 2 Deflagration in a Confined Volume," *Flow, Turbulence and Combustion,* vol. 101, no. 1, pp. 123-137, 2018.

[34] S. S. Vasu, D. F. Davidson, and R. K. Hanson, "Jet fuel ignition delay times: Shock tube experiments over wide conditions and surrogate model predictions," *Combustion and Flame,* vol. 152, no. 1, pp. 125-143, 2008.

[35] N. J. Killingsworth, V. H. Rapp, D. L. Flowers, S. M. Aceves, J.-Y. Chen, and R. Dibble, "Increased efficiency in SI engine with air replaced by oxygen in argon mixture," *Proceedings of the Combustion Institute,* vol. 33, no. 2, pp. 3141-3149, 2011.